Modeling hydrogen in $CuInSe_2$ and $CuInS_2$ solar cell materials using implanted muons

J. M. Gil, P. J. Mendes, L. P. Ferreira, H. V. Alberto, R. C. Vilão, and N. Ayres de Campos
Departamento de Física, Universidade de Coimbra, P-3000 Coimbra, Portugal

A. Weidinger and Y. Tomm
Hahn-Meitner Institut Berlin, Glienicker Strasse, 100, D-14109 Berlin, Germany

Ch. Niedermayer
University of Konstanz, Faculty of Physics, D-78434 Konstanz, Germany

M. V. Yakushev and R. D. Tomlinson
Department of Electronic and Electrical Engineering, University of Salford, Salford M5 4WT, United Kingdom

S. P. Cottrell and S. F. J. Cox
ISIS Facility, Rutherford Appleton Laboratory, Chilton, Didcot, Oxon OX11 0QX, United Kingdom
(Received 19 June 1998; revised manuscript received 5 October 1998)

Muon spin rotation experiments on $CuInSe_2$ and $CuInS_2$ were performed in the context of a study on the effect and behavior of hydrogen on chalcopyrite solar cell materials. The microscopic information delivered by implanted positive muons can be applied to the hydrogen case by analogy. It was found that the major fraction of the muons is in a diamagnetic environment but, at low temperatures, a fraction of 5–10 % has a paramagnetic surrounding. In $CuInSe_2$ the site of the diamagnetic muon is tentatively assigned to the antibonding site close to Se and the onset of muon diffusion on a microsecond time scale is observed between 200 and 250 K. The pre-exponential factor for the hop rate and the activation energy are $\nu_0 = 3.4 \times 10^{10}$ s^{-1} and $E_a = 220$ meV. Above 250 K trapping occurs. The diffusion behavior in $CuInS_2$ is similar, but the onset is shifted by 50 K to higher temperatures. [S0163-1829(99)00704-3]

I. INTRODUCTION

Chalcopyrites like $CuInSe_2$, $CuInS_2$, and derivatives obtained by partial replacement of In by Ga are promising solar cell materials. Energy conversion efficiencies of up to 17% have been obtained.[1] However, large area solar cells of these materials, as would be the case for industrial production, show a much lower efficiency, mainly due to the large presence of defects.

In solar cells made of amorphous silicon or indium phosphide, hydrogen is either an essential part of the system or is used to improve the performance of the cells.[2,3] The effect of hydrogen in the chalcopyrite materials is only now beginning to receive attention.[4–6] Experimental information on the local structure and electronic configuration of isolated hydrogen in these materials is in general difficult to obtain due to the usually low concentration of hydrogen involved. Muon spin rotation (μSR) can provide information on these configurations as well as on local electronic structure, because the muon can be regarded as a proton analogue or ''light isotope'' of hydrogen.[7]

Site determinations for the muon are made via the depolarization rate of the muon spin due to the magnetic moments of the surrounding nuclei. The resulting local-field distribution at the muon site has a strong dependence on the distances of the muon from these moments and on the orientation of an external field with respect to the crystallographic axes. Thus by measuring the depolarization rate of the muon spin in an external field for different orientations of those axes, the site of the muon can be determined.[8,9] However, this method is strictly applicable only if additional interactions such as quadrupole or hyperfine interactions can be decoupled in an external field. In the present case no decoupling effect was observed experimentally, thus this point remains somewhat uncertain, but valuable information could nevertheless be deduced from the data.

The diffusion behavior of the muon can be derived from the motional narrowing of the μSR line in transverse-field measurements or from the correlation time in zero-field measurements. With due regard to the large isotopic mass ratio ($m_{\mathrm{Mu}}/m_{\mathrm{H}} \approx 1/9$) this also illuminates the question of hydrogen diffusion.

II. EXPERIMENTAL DETAILS

The $CuInSe_2$ samples consisted of single crystals with dimensions of approximately 1.5 cm^2 area and $\geqslant 3$ mm thickness, produced by the vertical Bridgman technique.[10] Two *p*-type and one *n*-type crystals were used. The orientation of the crystals was determined by x-ray diffraction. The carrier concentration of the *p*-type samples at room temperature was of the order of 5×10^{16} cm^{-3}, and that of the *n*-type sample was of the order of 1×10^{16} cm^{-3}.

The $CuInS_2$ sample consisted of crystallites with dimensions of one to several millimeters in each direction. They were prepared in a closed quartz ampoule by chemical-vapor deposition under a temperature gradient. The material ob-

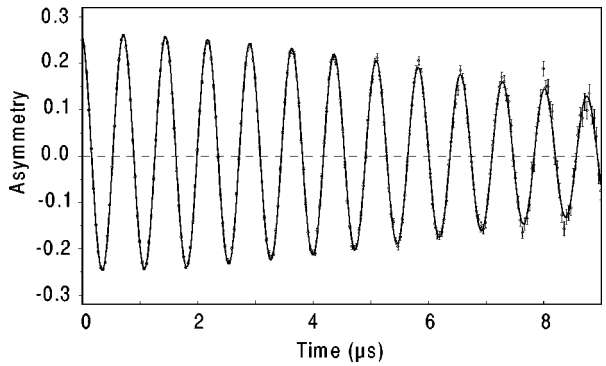

FIG. 1. Transverse-field μSR spectrum for a *n*-type $CuInSe_2$ sample at 100 K and 100 G. The solid line is a fit to a Gaussian-damped cosine function. The frequency corresponds to the Larmor precession due to the applied external field.

tained was *p*-type with a carrier concentration in the order of typically 10^{14} cm^{-3}.

Transverse-field μSR experiments were performed at the Paul-Scherrer Institute in Switzerland and zero-field experiments at the Rutherford Appleton Laboratory, in England. Typical examples of μSR spectra are displayed in Figs. 1 and 2. The transverse-field data (Fig. 1) were analyzed by fitting one or more cosine functions of time, together with a damping or envelope function according to[11]

$$P(t)=\exp\left(-\frac{1}{2}\sigma^2t^2\right) \quad \text{(static)}, \tag{1}$$

$$P(t)=\exp\left\{-\sigma^2\tau_c^2\left[\exp\left(-\frac{t}{\tau_c}\right)-1+\frac{t}{\tau_c}\right]\right\} \quad \text{(dynamic)}, \tag{2}$$

where σ is the static Gaussian depolarization rate and τ_c is the correlation time. The zero-field data (Fig. 2) were analyzed by fitting one or more static or dynamic Kubo-Toyabe functions of the form[12]

$$p_z(t)=\frac{1}{3}+\frac{2}{3}(1-\Delta^2t^2)\exp\left(-\frac{1}{2}\Delta^2t^2\right) \quad \text{(static)}, \tag{3}$$

$$P(t)=p_z(t)\exp(-\nu t)+\nu\int_0^t p_z(t')\times\exp(-\nu t')P_z(t-t')dt' \quad \text{(dynamic)}, \tag{4}$$

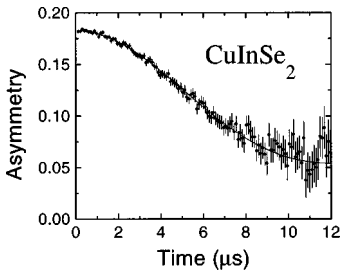

FIG. 2. Zero-field μSR spectrum for a *p*-type $CuInSe_2$ sample at 100 K. The solid line is a fit to a static Kubo-Toyabe depolarization function and an undamped background signal.

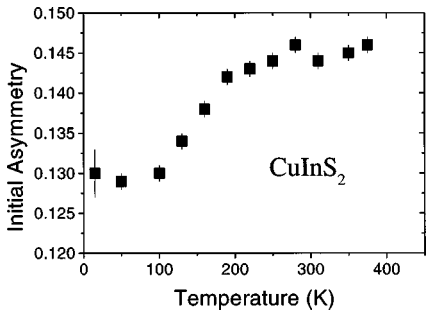

FIG. 3. Initial asymmetry of the zero-field μSR signal as a function of temperature for $CuInS_2$. The decrease at low temperature indicates a missing fraction due to the formation of an undetected muonium state.

where Δ gives the rms width of the local-field distribution and $\nu=1/\tau_c$ is the hop rate.

III. EXPERIMENTAL RESULTS AND DISCUSSION

The transverse-field data (Fig. 1) show a μSR frequency corresponding to a Larmor precession in the external magnetic field, indicating that the muon is in a diamagnetic state. The diamagnetic fraction accounts, at low temperatures, for approximately 90% to 95% of the total implanted muons but there is a small missing fraction, which in the $CuInS_2$ sample could be identified as a rapidly relaxing component and is therefore assigned to a paramagnetic center. The initial asymmetry, which shows the effect of the missing fraction at temperatures below 150 K, is displayed in Fig. 3. In the following only the diamagnetic majority component will be discussed further.

A. Muon site in the chalcopyrite structure

In order to characterize the site of the muon in the crystal structure we applied the common method of evaluating the dipolar interaction of the muon with the neighboring nuclei.[8,9] For this method to be applicable, additional interactions such as quadrupole or hyperfine interactions have to be decoupled so that the Van Vleck values can be used. On $CuInSe_2$ *p*-type single crystals oriented with the main crystallographic axes $\langle 112\rangle$, $\langle 100\rangle$, and $\langle 110\rangle$ parallel to the magnetic field, the muon spin depolarization rate σ was measured at 10 K (where no motion is apparent) as a function of the transverse magnetic field up to 0.6 T. The results are shown in Fig. 4. The figure is presented in logarithmic scale as usual for convenience. No sizeable variation of σ was found neither with field nor with orientation that would allow the identification of a decoupling. The values found were always very close to an average value of 0.14 μs^{-1}. The measured zero-field Kubo-Toyabe width (not shown here) is slightly larger than the transverse-field width as expected from quantum mechanics.

Calculations of the depolarization rate expected in the high-field (Van Vleck) limit were made for a muon in the (undistorted) $CuInSe_2$ lattice at different sites along the diagonal of the half unit cell. The unit cell of $CuInSe_2$ is presented in Fig. 5, where the referred interstitial sites are depicted as small white spheres. In tetrahedrally coordinated systems like Si or GaAs the muon sites have been found to

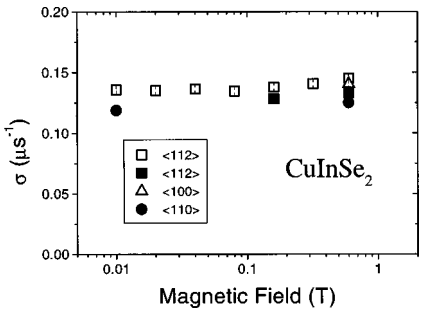

FIG. 4. Transverse-field depolarization rates σ for two different p-type $CuInSe_2$ single crystals as a function of external field. The respective results are represented by open and closed symbols. The crystallographic orientations with respect to the external field are indicated in the figure. The error bars are about the size of the symbols.

be along the bond directions, that is on the diagonal of the unit cell.[13,14] The bond center (BC), the tetrahedral (T), and the antibonding (AB) sites were considered as possible muon sites. In a two-component crystal lattice, two tetrahedral and two antibonding sites can be distinguished, depending on the surrounding atomic species. Since the present system is also tetrahedrally coordinated it is reasonable to assume that the muons are also at sites along this axis, which corresponds to the $\langle 112 \rangle$ direction in the chalcopyrite unit cell.

The calculations were made using the averaged (weighted with the isotope abundance) nuclear moments of the Cu and In nuclei and assuming zero nuclear moment at the Se sites, i.e., the effect of the ^{77}Se nuclei (abundance 7.6%) was neglected, the other Se isotopes having zero moments.

Since the muon can stop at any of the crystallographic equivalent sites of a certain type (in our assumption belonging to the different diagonals in the half unit cell) the results of the respective calculated depolarization rates have to be averaged, as crystallographically equivalent sites are generally inequivalent with respect to the external field. Note that this averaging must be performed incoherently since it corresponds to different muons in unit cells which are far apart. The appropriate fractions of muons stopping at each of these sites could in principle be distinguished in the experimental

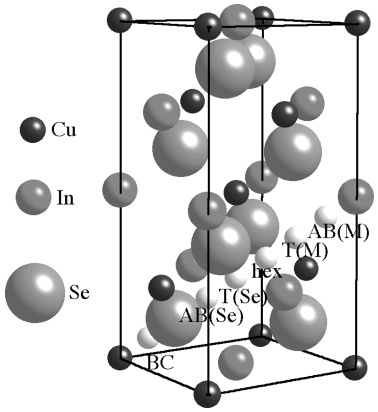

FIG. 5. $CuInSe_2$ unit cell. Possible muon sites on the diagonal of the half unit cell are indicated as small white spheres, and labeled as follows: bond center (BC), antibonding near Se (AB_{Se}), antibonding near metal (AB_M), tetrahedral near Se (T_{Se}), tetrahedral near metal (T_M), hexagonal (hex).

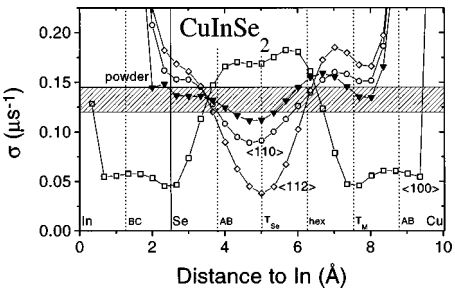

FIG. 6. Theoretical calculation of the depolarization rate σ in the high-field (Van Vleck) limit for a muon in the $CuInSe_2$ lattice at different sites along the diagonal of the half unit cell, from an In, via a Se, to a Cu site. The bond center (BC), the antibonding (AB), the tetrahedral (T), and hexagonal (hex) interstitial sites are indicated. There exist two AB and two T sites, depending on whether the chalcogens or the metals are the nearest neighbors. σ values were calculated for the external field applied along the $\langle 112 \rangle$, $\langle 110 \rangle$, and $\langle 100 \rangle$ axes, respectively. All equivalent positions in the unit cell were taken into account and the results were averaged. The dashed area indicates the range of σ values observed experimentally.

spectra but only with extremely high acquisition times. The result is different from that expected for a fast cage motion of a muon sampling these sites in the same unit cell. Calculations were made for sites along a $\langle 112 \rangle$ direction from an In at one corner via a Se towards Cu at the other corner of the half unit cell and from Cu via Se towards In. The four sites on the crystallographic equivalent directions were always taken into account.

Figure 6 presents these results for the In towards Cu direction considering an external field applied along the $\langle 100 \rangle$, $\langle 110 \rangle$, and $\langle 112 \rangle$ axes of a single crystal and for a polycrystalline sample. We notice that in the Van Vleck limit, a clear distinction of sites via the characteristic behavior of the σ values can be made. For example, at the bond center (BC) and at the tetrahedral sites (T_{Se} and T_M) which correspond to the BC and T sites occupied by the muon in elemental and III-V semiconductors, very strong orientation dependencies of the σ values are predicted, in contrast to our experimental finding referred above that the σ values are practically the same in all three external field directions. The experimental result of no orientation dependence of σ and a value around 0.14 μs^{-1} (dashed area in Fig. 6) is well matched at a site close to AB in Fig. 6. Thus an assignment of the muon site to this position is fully consistent with the data.

A similar crossing of the σ values of the different orientations occurs near the hexagonal (hex) site in Fig. 6. However, both theory and experiment in other semiconductors indicate that the hexagonal site is more like a saddle point rather than a minimum in the potential energy surface and therefore is unlikely to be a candidate for the muon site in the present case. We also performed calculations in the direction along the Cu-Se bond. Due to the fact that we assigned no nuclear moments to the Se atoms in the calculations, the predicted σ values are just the mirror image about the T_{Se} line in Fig. 6. In particular, the antibonding site along a Cu-Se bond is equivalent to the hexagonal site in Fig. 6. Although these predicted σ values do not fit as well as those for the In-Se anti-bonding site, they are close enough to the

experimental values to be acceptable. Thus, the AB sites, both those along a In-Se bond as well as those along a Cu-Se bond, are consistent with experiment as well as a mixture of the two.

The application of the Van Vleck theory relies on the assumption that the external magnetic field determines the quantization axis for the nuclear spins, i.e., that the quadrupolar (or other spin) interaction can be decoupled. The quadrupole interaction at the Cu and In nuclei in pure $CuInSe_2$ is known from nuclear quadrupole resonance (NQR) measurements.[15] Due to the noncubic local structure this interaction is nonzero, but the strength is rather small and can easily be decoupled at 0.6 T (the ratio of ω_B/ω_E, which is a measure of the magnetic versus electric interaction,[8] is 107 for ^{63}Cu and 280 for ^{115}In at 0.6 T). Besides this crystal-field effect, an induced quadrupole interaction due to the presence of the muon could exist. The magnitude of this interaction and the distribution over the different nuclei will very much depend on the site of the muon in the unit cell and cannot be estimated with our present knowledge.

Experimentally, we find no decoupling effect for magnetic fields up to 0.6 T. If we assume that the muon resides at the antibonding site as discussed above, the averaging over the crystallographic equivalent positions may smear out the spin orientation effects and lead to a field and orientation-independent depolarization rate consistent with experimental observation. The alternative assumption that a strong, muon-induced interaction, which cannot be decoupled is responsible for the constancy of the depolarization rate also points to the AB site assignment since in this case the expected magnitude of σ would be close to the calculated polycrystalline value, which again fits best for the antibonding site.

The AB site assignment gets support from a recent calculation of the hydrogen potential energy in GaN.[16] There the authors came to the conclusion that in this more ionic crystal the antibonding site is preferred over the bond centered and tetrahedral sites observed in the covalently bonded Si or GaAs systems. It can be assumed that this argument is also valid for the present system.

In a polycrystalline $CuInS_2$ sample the depolarization rate σ was found to be 0.14 μs^{-1} at low temperatures. This similarity with the values obtained for $CuInSe_2$ and the fact that the calculations give approximately the same values as in Fig. 6 (S and Se having similarly weak nuclear magnetism) suggests that the muon sites are equivalent in the two compounds.

B. Muon diffusion

Figure 7 shows the transverse-field depolarization rate σ for a *p*- and a *n*-type single crystal as a function of temperature, obtained by fitting the data with formula (1). The decrease of σ above 200 K is attributed to motional narrowing at the onset of diffusion. As can be seen from Fig. 7, the two samples behave very similarly in this temperature range, indicating that the electronic structure of the muon state and the diffusion behavior are similar in these two differently doped samples. In GaAs,[17] a different diffusion behavior has been observed for heavily doped *p*- and *n*-type samples, which was attributed to the formation of Mu^+ in the *p*-type and a Mu^- in the *n*-type material and a different diffusion of

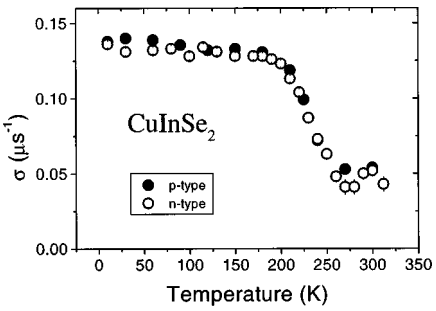

FIG. 7. Transverse-field depolarization rate σ for a *p*- and a *n*-type single crystal as a function of temperature.

Mu^+ and Mu^-. However, the formation of Mu^-, counterpart of the interstitial hydride ion, is guaranteed only in heavily doped *n*-type samples and probably does not occur in our samples. We assume that the data in Fig. 7 correspond to Mu^+ in both cases,[13,14,18] counterpart of the interstitial proton.

The motional narrowing region in Fig. 7 was analyzed with formula (2), taking for σ the low-temperature value and holding it constant. The inverse correlation times $\nu = 1/\tau_c$ extracted from these data are displayed as hop rates in Fig. 8. In addition, hop rates extracted from zero-field measurements according to formula (4) are included. They agree well with the data from the transverse-field measurements. The linear region in this Arrhenius plot is fitted with an attempt frequency of $\nu_0 = 3.4 \times 10^{10}$ s^{-1} and an activation energy of 220 meV. In GaAs and InP, the onset of motional narrowing was observed in a similar temperature range for *p*-type and not too heavily doped *n*-type samples.[17,19] Thus, the diffusion behavior of the muons in the present chalcopyrite samples is similar to that in the III-V compounds.

The fact that the hop rate does not keep increasing above 250 K is interpreted as an indication of trapping, as is observed also in GaAs and InP at elevated temperatures.[17,19] The trapping at these higher temperatures is also evidenced by the fact that zero-field measurements cannot be well fitted above 250 K with the dynamic Kubo-Toyabe formula (4), but rather require the static formula (3) with a low value of Δ.

Figure 9 shows the muon hop rate data for polycrystalline $CuInS_2$. We have purposely chosen the same scale as in Fig.

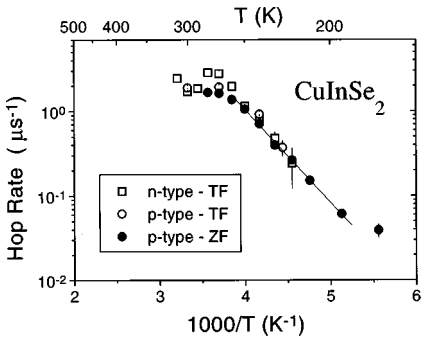

FIG. 8. Arrhenius plot of the hop rate in the region of motional narrowing for *n*-type (in transverse-field) and *p*-type (in transverse- and zero-field) $CuInSe_2$ crystals. The straight line is a fitting to an activated hop rate and gives an attempt frequency of $\nu_0 = 3.4 \times 10^{10}$ s^{-1} and an activation energy of 220 meV.

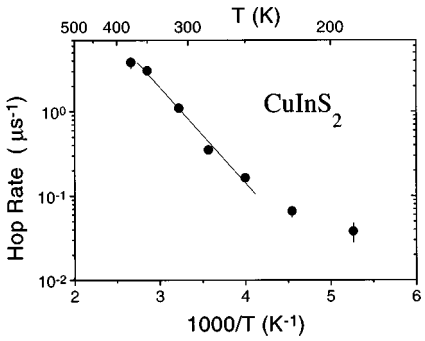

FIG. 9. Arrhenius plot of the hop rate in the region of motional narrowing for *p*-type $CuInS_2$ crystallites, measured in zero-field. The straight line is a fitting to an activated hop rate and gives an attempt frequency of $\nu_0 = 4.9 \times 10^9$ s^{-1} and an activation energy of 225 meV.

8 to express more clearly the difference in the data. It can be seen that the increase of the hop rate is shifted to considerably higher temperature (by about 50 K) showing that the diffusion is slower in the sulfide than in the selenide (it seems unlikely that the effect is due to single crystal versus polycrystalline structure since the muon diffusion is a local effect in the crystallites). Qualitatively, the more localized electron wave function at the lighter sulfur compared to the heavier selenium could lead to a stronger binding of the muon and therefore retard diffusion as the temperature is increased.

Recent measurements of hydrogen diffusion, derived from profile broadening in hydrogen implanted $CuInSe_2$ samples,[20] gave diffusion coefficients five orders of magnitude lower than the ones derived for the muon from the present data. Although this may be an extreme example of the effect of isotopic mass, it seems more likely to indicate that the measured hydrogen data relate to trap or cluster governed diffusion, whereas the muon data come closer to representing the intrinsic diffusion of an interstitial hydrogen like atom in the perfect lattice. These aspects deserve theoretical modeling.

IV. CONCLUSION

These first μSR studies of the chalcopyrites $CuInSe_2$ and $CuInS_2$ cover the temperature range up to just above room temperature and a selection of representative samples. We find that the muon is predominantly (90–95 %) in a diamagnetic state, most likely the positively charged defect center Mu^+, a model for the interstitial proton. For a small fraction of muons a signal consistent with a paramagnetic state (presumably the neutral center Mu^0, counterpart of trapped atomic hydrogen) is observed at low temperature. Linewidth analysis of the diamagnetic fraction as a function of the crystal orientation and external magnetic-field strength suggests that the muon is bound to Se along a metal-Se bond opposite to the metal site (i.e., the antibonding site). For this situation the required averaging over the crystallographic equivalent positions smears out the orientation dependence and gives rise to the observed insensitivity of σ to the orientation and field strength. Motional narrowing indicates the onset of diffusion above 200 K. The observed hop rates in this region are similar to those observed for the positive ion Mu^+ in GaAs and InP. Above 250 K the diffusion appears to be limited by trapping. In the corresponding sulfide compound the diffusion sets in at a temperature 50 K higher.

ACKNOWLEDGMENTS

We thank J. A. Paixão and A. Matos Beja for x-ray sample orientations. We also thank Pierre Dalmas de Réotier for allowing the use of his computer code for nuclear depolarization rates calculations. This work was supported by PRAXIS XXI (Portugal, PCEX/P/FIS/16/96), EU TMR program for Large Scale Facilities (research at ISIS), EPSRC (UK, GR/L62757), and INTAS (no. 634).

[1] M. A. Green, K. Emery, K. Bücher, and D. L. King, Prog. Photovoltaics **4**, 59 (1996).
[2] H. C. Neitzert and M. Briere, J. Non-Cryst. Solids **115**, 75 (1989).
[3] B. Chatterjee, S. A. Ringel, and R. Hoffman, Jr., Prog. Photovoltaics **4**, 91 (1996).
[4] K. Kushiya, H. Hakuma, H. Sano, A. Yamada, and M. Konagai, Sol. Energy Mater. Sol. Cells **35**, 223 (1994).
[5] M. V. Yakushev, H. Neumann, R. D. Tomlinson, P. Rimmer, and G. Lippold, Cryst. Res. Technol. **29**, 417 (1994).
[6] K. Töpper, J. Bruns, R. Scheer, M. Weber, A. Weidinger, and D. Bräunig, Appl. Phys. Lett. **71**, 482 (1997).
[7] S. F. J. Cox, J. Phys. C **20**, 3187 (1987).
[8] O. Hartmann, Phys. Rev. Lett. **39**, 832 (1977).
[9] M. Camani, F. N. Gygax, W. Rüegg, A. Schenck, and H. Schilling, Phys. Rev. Lett. **39**, 836 (1977).
[10] R. D. Tomlinson, Sol. Cells **16**, 17 (1986).
[11] A. Abragam, *The Principles of Nuclear Magnetism* (Oxford University Press, Oxford, 1961).
[12] R. S. Hayano, Y. J. Uemura, J. Imazato, N. Nishida, T. Yamazaki, and R. Kubo, Phys. Rev. B **20**, 850 (1979).
[13] S. F. J. Cox and R. L. Lichti, J. Alloys Compd. **253-254**, 414 (1997).
[14] K. H. Chow, R. F. Kiefl, W. A. MacFarlane, J. W. Schneider, D. W. Cooke, M. Leon, M. Paciotti, T. L. Estle, B. Hitti, R. L. Lichti, S. F. J. Cox, C. Schwab, E. A. Davis, A. Morrobel-Sosa, and L. Zavieh, Phys. Rev. B **51**, 14 762 (1995).
[15] K. D. Becker and S. Wagner, Phys. Rev. B **27**, 5240 (1983).
[16] J. Neugebauer and C. G. Van de Walle, Phys. Rev. Lett. **75**, 4452 (1995).
[17] K. H. Chow, S. F. J. Cox, E. A. Davis, S. R. Dunsiger, T. L. Estle, B. Hitti, R. F. Kiefl, and R. L. Lichti, Hyperfine Interact. **105**, 309 (1997).
[18] K. H. Chow, Hyperfine Interact. **105**, 285 (1997).
[19] R. L. Lichti, S. F. J. Cox, C. Schwab, T. L. Estle, B. Hitti, and K. H. Chow, Hyperfine Interact. **105**, 333 (1997).
[20] D. Fink, J. Krauser, G. Lippold, M. V. Yakushev, R. D. Tomlinson, A. Weidinger, K. K. Dwivedi, S. Gosh, and W. H. Chung, Radiat. Eff. Defects Solids **145**, 85 (1998).